

Scouring of Bridges: Numerical and Experimental Studies

Chaymae NAAZA^{1*}, Abdellah EL BARKANY¹, Rafik ABSI², Ikram EL ABBASSI²

¹Mechanical Engineering Laboratory, Faculty of Science and Techniques,
Sidi Mohammed Ben Abdellah University, Fez, Morocco

²ECAM-EPMI, 13 Boulevard de l'Hautail, 95092, Cergy Pontoise Cedex, France

^{1*}Corresponding Author : Chaymae.naaza@usmba.ac.ma

Received: 07 November 2022

Revised: 15 January 2023

Accepted: 19 February 2023

Published: 25 February 2023

Abstract - Scour is classified as a very complex natural phenomenon that appears in front of piles and abutments of bridges. Experimental methods in laboratories were developed in order to estimate the depth of the scour hole taking into consideration different parameters such as hydraulic, geotechnical and structural parameters. These models are based on experimental methods in laboratories and are affected by oversimplified setups, which lead to inaccurate results. Engineering advanced methods such as the Computational Fluid Dynamics (CFD) are extensively used to solve complex models in industrial and engineering applications. Among the wide range of known flow calculation codes, CFX, Fluent, Numeca, Star-CD, Openfoam etc.. are mentioned. The objective of this paper is to treat the modelling methods and the differences between them as well as the equations governing the flows and widely used in the Computational Fluid Dynamics (CFD).

Keywords - Bridge, CFD, Code fluent, Horseshoe vortex, Scour.

1. Introduction

In 1967, Ohio Bridge collapsed when it was congested with rush-hour traffic, resulting in the death of 46 people [1]. Most recently, the I-35W Bridge across the Mississippi River collapsed, causing 13 deaths and 145 injuries.[2] In the United States, during the period between 1989 and 2000, 503 of bridges collapsed causing much material damage what drove researchers and engineers to study the causes of the collapse of these bridges. [3] On the night of 4 March 2001, the Hintze Ribeiro Bridge made of steel and concrete collapsed in Portugal, killing 59 persons, among them three cars crossing the Douro river. According to authorities, the collapse was due to uncontrolled sand erosion, which affects the stability of the bridge's foundations. [4] Local scour is the removal of materials around bridge foundations under the erosive action of water which leads to their exposure and therefore to the instability of the hydraulic structure.[5] Many investigations were made by researchers in order to ensure regular monitoring of scouring. On one hand, many empirical equations are proposed in the literature [6,7] and are based on experimental methods in laboratories thing which makes their results unreliable. [8,9] On the other hand, numerical models are used to simulate the turbulence and estimate the impact of the Horseshoe Vortex among the piers.[10] Local scour is caused by the apparition of the Horseshoe Vortex at the base of hydraulic structures due to the accumulation of water in the junction between the bed and the pier [11] as shown in the figure 1 below. Local scour around piers have been a subject of interest for many researchers. Certainly, the physical model gives reliable

results except that the problem of scale limits it; in addition, it is hard to keep Froud number (Fr) and Reynolds number (Re) constant. [12]

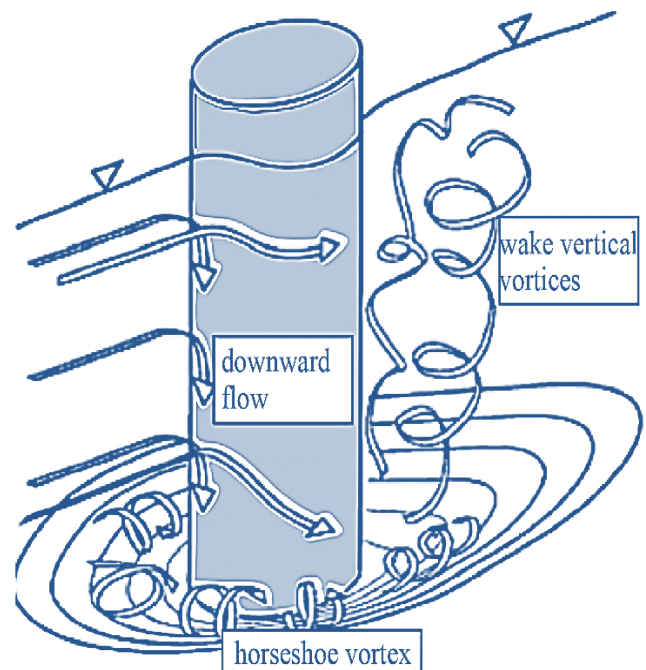


Fig. 1 Horseshoe vortex around circular pier

The depth and location of scour hole depends on erosion process and the transport of sediments that depend on materials types, the velocity of flow, and the shape



of the pile.... The gathering of these parameters is difficult to implement in a numerical simulation. Many models have been used in the context of certain research, but they are still unclear. The main objective of this paper is to discover physical models and numerical ones and compare between them.

2. Experimental Studies

Scour appears under different conditions, which make it hardly predictable and simulated. Before, the increase of the power of computers and the development of numerical methods the three-dimensional flow was followed in laboratories.

2.1. Scour Downstream Dams

Many researchers studied local scour downstream barrages. In this condition, scour is treated as a two-dimensional scour as the variation of flow, and scour depth in the third direction are neglected compared to the other two directions.

(Balachandar et al., 2000)[13] studied scour under a dam gate and found that scour occurs in two main phases. The first one is characterized by the development of the scour hole when the jet is directed towards the bed, and the second is a refilling phase when the scour hole is already filled by the materials eroded. The jet is directed towards the free surface. Both phases rotated until equilibrium is reached.

(Breusers, H (1965; 1967)) [14] suggested an empirical equation Eq. (1) to calculate the scour depth as a function of time after studying experimentally the scour hole in a non-cohesive bed.

$$d_s = h \left(\frac{t}{T_s} \right)^{0.38} \quad (1)$$

where d_s the maximum scour depth, h is the upstream water depth, T_s is the time at which $d_s = h$

(Chattarjee et al.; 1980; 1994) [15,16] measured the scour hole in an erodible bed generated by a flooded jet coming out from a sluice opening over an apron. An empirical relation between the maximum scour depth and time was also established. They also measured The flow velocity of the submerged jet. The equilibrium is reached.

2.2. Scour Around Vertical Cylinders

Local scouring can occur as Clearwater scour or Live bed scour: In effect, the first regime is produced when the sediments are at rest, i.e. they do not move around the structure, in the second regime, sediment transport occurs from upstream to downstream of the pile. [58] The two types of scour have been investigated by many scientists. [18,19] Based on many experiences and field measurements, (Melville et al.;2000;1997;1988) [20–22] Made detailed studies in order to make this phenomenon

more comprehensive, they conclude experimentally that the generation of characterizes scour the Horseshoe vortex in the scour hole after the appearance of the downward flow in front of piles.

Van Rijn (2018) [23] made different experiences on piers and used many equations to calculate the depth of scour hole and conclude the differences between the main used equations.

Whitehouse (2004)[24] made experiences on monopole and three different large marine foundations in currents and waves then he studied the maximum scour depth produced by waves and steady currents. He provided good indications of the potential scour that can be developed under current conditions and 'live bed' waves or current regimes and confirmed that Foundations are less sensitive to this natural phenomenon in areas where waves dominate.

(Breusers et al., 1977) [25] analyzed field data and laboratory experiments and found that maximum scour depth depends on many parameters such as shape of the pile, velocity of the flow, angle of attack and the depth of the flow. As a conclusion, they estimate the scour depth through these parameters.

(Oscar et al., 2008) [56] presented experiments aimed at studying the characteristics of the development of scour holes around a circular cylinder embedded in the sand. In the experiment, the measurements of scour hole were taken by a laser distance sensor (LDS) in different azimuthal half-planes in order to study the spatiotemporal variation of geometric properties of the developed scour hole. These measurements show that the scour begins upstream and on the sides of the cylinder then surrounds it and spreads to the region behind it. The slopes of the developing scour holes exhibited three regions with different slopes, which were attributed to the action of the vortices.

Boujia (2019) [5] proposes a technique for continuous monitoring of scour using sensor buried in two types of soil: dry sand and a soft clayey soil. Some issues were investigated: the effect of soil type, the effect of the geometry and materiel of the sensor. The erosion of the soil around the pile causes the variation of the height of the rod, and consequently of its vibration frequency. By correlating the vibratory response of the rod to its free height, the scour depth around the pile can be determined.

(Sumer et al.; 1998; 2001) [27,28] studied scour around group of vertical piles and a large vertical one. For two or three piles, different configurations have been studied. They conclude that scour depth is influenced by the spacing between piers and the side-by-side configuration increase the depth scour while the in-line layout will decrease it.

3. Comparative study of the different cfd methods

3.1. Numerical Studies

In recent years and with the ever-increasing capabilities of computer hardware and software, CFD (Computational Fluid Dynamics)[17,40,44,54,55] has been widely used to solve flow equations in industrial and environmental applications. Significant progress has been made recently in the use of numerical simulation to study flow and scour around hydraulic structures. The development of numerical models to predict sediment transport is a challenge as simulations require more computer resources. Numerical methods, and to cope with this situation, have been developed, and in parallel, the computer resources themselves have been multiplied.

The numerical modeling is essentially based on two elements: A hydraulic module and a morphological module. The first one is used to solve the Navier-Stokes equations for the flow field, and the second one to deal with the bed erosion and the sediment transport. The sediment-laden flow is treated as a two-phase flow including liquid phase and sediment phase or as a one-phase flow in which water and sediments are modelled as a mixture. Multiphase models are categorized into the Euler-Euler type and the Euler Lagrange type. The Euler-Lagrange model treats the sedimentary phase as movements of a number of individual particles. This approach succeeds in capturing individual dynamics and collective natural sand grains. (Li et al., 2014) [29] Developed a 3d Euler Lagrange Model to predict scour around offshore structures. The model kept the physical properties of each phase, and it represents the vortices of the wake side of the cylinder. Many other models of the Euler Lagrange type have been studied recently.[30,31]. The disadvantage of this approach is that it requires a large number of particles, which in turn requires extensive computing resources. The Euler Euler Approach describe the fluid and sediment phases. It is usually very complicated because it needs to solve the equations of continuity and momentum for the two phases and also to describe the turbulence characteristics for both fluid and sediments as confirmed (Chen et al., 2011).[32] Many models have been established to treat the nondilute transport of sediments in open channels.[33] (Li et al., 2008) [34] developed a biphasic numerical model using a one-equation turbulence closure in order to predict sediment transport under oscillating laminar flow conditions. Single-phase flow models are limited in the particle motion side, fluid/particle and particle/particle interactions are not taken into account and this at high concentrations of sediments generally near the bed. In these models, the interaction between dispersed phases and continuous phases are neglected and advection-diffusion model is solved in order to determine the volumetric concentration of sediments. In the studies of (Liang et al., 2005) [35] and (Roulund et al., 2005) [36] the advection-diffusion model has been strongly applied to numerous numerical studies of scour problems.

3.2. The Turbulence Model

A turbulent flow is composed of "fluid threads" which, instead of keeping their individuality by sliding only on each other as in a laminar flow, exchange fluid particles between them. The flow regime is characterized by a dimensionless number called the Reynolds number Re . There are three main areas of simulation: direct numerical simulation (DNS), large-eddy simulation (LES) and purely statistical modelling [37]. According to the theory of Kolmogorov, the turbulent agitation is composed of vortex structures whose sizes are continuously distributed over a range of length scales, bounded by the geometry of the flow, and below by the Kolmogorov scale, the seat of viscous dissipation.

3.2.1. DNS

Direct Numerical Simulation (DNS) consists in solving explicitly all the scales of turbulence by solving the Navier-Stokes equations numerically. The resulting three-dimensional and unsteady field describes reliably and accurately the turbulent agitation.[38] The DNS is conceptually the most straightforward, and easiest approach however the computational cost is incredibly high because the resolution of the smallest dissipative scale needs very fine computational meshes. Another drawback of this approach is that the high fines of the turbulence structure require the prescription of initial and boundary data at an important level, which is not without serious difficulties at times. In addition, DNS solves all scales of turbulence, and its computational cost is proportional to Re^3 . A series of direct numerical simulations has been investigated by (Wissink et al., 2008)[39] around a circular cylinder at Re from 3300 to 3900 and with the maximum number of meshes of about 5×10^8 .

3.2.2. RANS

In realistic flows, an alternative is to be interested only in the average quantities and thus to obtain the system of equations verified by these quantities. To do this, it is necessary to apply the mean operator on the instantaneous equations by practicing the Reynolds decomposition on the unknowns of the problem. The new equations obtained are called averaged equations. The RANS simulations only need to represent the gradients present in the mean field, the rest being modeled. The main disadvantage of these methods comes from the modeling of the turbulence. The modeling is often based on simplifications which are only true under certain assumptions. The flow field has been studied around circular piers using the RANS approach by many researchers, such as (Majumdar et al., 1989)[57] (Nagata et al., 2005)[41] and (salaheldin et al., 2004).[42]

3.2.3. LES

Large Eddy Simulation consists in solving the averaged Navier-Stokes equations. The contributions of the largest scales of turbulence are computed and only the smallest structures are modeled. Concerning the solved equations, the solved quantities are filtered, and only the structures larger than the characteristic size of the filter are

solved. The effect of the smallest structures of the turbulence appears through terms that require a modeling.

3.2.4. Statistical Approach

Models based on the statistical approach are the most common. They are based on the classical Reynolds decomposition into mean and fluctuating quantities.

3.2.5. DES

Detached Eddy Simulation is a combination between RANS and LES that was proposed in 1997. According to spalart (2009)[43], It is about using LES far from the boundary layers and near the walls RANS; this hybrid approach was introduced in order to reduce the computational resource consumption of LES and DNS, the RANS near the walls requires less mesh than LES or DNS, knowing that the dominant quantity is the average one in this area. This table represents the major differences between the different numerical modelling methods.

Table 1. Major differences between Numerical Modeling Methods

	DNS	RANS	LES
Dependence of Reynolds Number	Strong	weak	Medium
Computing time	Very long	Weak	Medium
Mesh	10 ¹⁶	10 ⁷	10 ^{11.5}

(Aghaee et al., 2010) [59] developed two numerical models for simulation of the turbulent flow around circular cylinders, the first one with the RANS approach and the second with the LES. As a result, the RANS needs a few grids for simulation, but it is still unable to show the horseshoe vortex and the Lee wake vortices around the bridge pier, unlike the LES method. Also, the shear stress in the LES approach is more intensive and extensive than in the RANS approach.

3.3. Governing Equations

The three-dimensional Navier-Stokes and continuity equations can be written for LES and RANS as follows :

$$\frac{\partial u_i}{\partial x_i} = 0 \tag{2}$$

$$\frac{\partial u_i}{\partial t} + \frac{\partial u_i u_j}{\partial x_j} = -\frac{1}{\rho} \frac{\partial P}{\partial x_i} + \vartheta \left(\frac{\partial^2 u_i}{\partial x_j^2} \right) + \frac{\partial \tau_{ij}}{\partial x_j} \tag{3}$$

Where $x_i = 1, 2, 3$ denotes the stream-wise, span-wise and vertical directions respectively, u_i : time-averaged or filtered velocity components in the mentioned directions, P time averaged or filtered pressure, ρ the fluid density, ϑ the kinematic viscosity of the fluid, and τ_{ij} Reynolds shear stresses or sub-grid shear stresses.

Where: $\tau_{ij} = -\rho u'_i u'_j$, u'_i : the fluctuating part of viscosity and $-\rho u'_i u'_j$: the Reynolds constraints

In order to estimate the Reynolds constraints, The fluent computational code proposes the standard $k - \epsilon$ model. This model assumes that the turbulence regime is fully established in the entire domain and that the effects of molecular viscosity are negligible compared to those of the turbulent viscosity. The turbulence field is thus introduced in term of kinetic energy k and its rate of dissipation ϵ . The equations governing k and ϵ can be written as follows:

$$\frac{\partial k}{\partial t} + \frac{\partial u_i k}{\partial x_j} = \frac{\partial}{\partial x_j} \left(\frac{\vartheta_t}{\sigma_k} \frac{\partial k}{\partial x_j} \right) + P - \epsilon \tag{4}$$

$$\frac{\partial \epsilon}{\partial t} + \frac{\partial u_i \epsilon}{\partial x_j} = \frac{\partial}{\partial x_j} \left(\frac{\vartheta_t}{\sigma_\epsilon} \frac{\partial \epsilon}{\partial x_j} \right) + C_{1\epsilon} \frac{\epsilon}{k} P - C_{2\epsilon} \frac{\epsilon^2}{k} \tag{5}$$

$$P = \vartheta_t \left(\frac{\partial u_i}{\partial x_j} + \frac{\partial u_j}{\partial x_i} \right) \frac{\partial u_i}{\partial x_j} \tag{6}$$

Where: ϑ_t is the eddy viscosity and is defined as:

$$\vartheta_t = C_\mu \frac{k^2}{\epsilon} \tag{7}$$

(Aghaee et al., 2010) (45) prescribed the five constants as: $C_\mu = 0.09$, $C_{1\epsilon} = 1.44$, $C_{2\epsilon} = 1.92$, $\sigma_k = 1$, $\sigma_\epsilon = 1.3$ and defined the Reynolds shears stress as :

$$\tau_{ij} = \vartheta_t \left(\frac{\partial u_i}{\partial x_j} + \frac{\partial u_j}{\partial x_i} \right) - \frac{2}{3} k \delta_{ij} \tag{8}$$

3.4. Examples of Numerical Simulation of Local Scour

Some of the most important and frequently referenced papers on numerical local scour simulation in recent years are briefly summarized below :

(Richardson and Panchang, 1998) [45] simulated the flow structures around a bridge pier with and without scour using FLOW3D with the $k-\epsilon$ RNG model. They found, after comparison with an experimental model, that the 3D hydrodynamic model simulates the complex flows around the bridge piers well.

Brørs (1999)[46] proposed a numerical simulation of flow and scour at pipelines. He used a $k-\epsilon$ turbulence closure model to calculate the flow field.

(Thanh et al., 2014) [47] used a numerical model to simulate the evolution of a scour hole developed around the bridge pier using FSUM based on a finite-difference method to solve the Reynolds averaged Navier-Stokes equations (RANS) and the equations for sediment concentration and bed morphology. They conclude after a comparison of numerical results with experimental data that the maximum scour depth appears at the two front edges of the pier.

(Tseng et al., 2000) [48] used the Large Eddy Simulations (LES) to conduct the numerical simulation of flow around square and circular piers. They found that the downward flow on the upstream face of the abutments and bridge piers exists and benefits the creation of the horseshoe.

(Sumer et al., 2002)[49] used a finite volumic hydrodynamic model in order to simulate the 3D flow around a pile. They were able to capture all the steps of scour process (the horseshoe vortex, the sediment transport, the shape of the scour hole). They also calculate the equilibrium scour depth and compare it with the measures made in the laboratory.

(Roulund et al., 2005) [36] conducted a numerical and experimental investigation of flow and scour around a circular pile exposed to a steady current. The flow was simulated using the hydrodynamic model EllipSys3D with a k- ω turbulence model, and the free surface effects were neglected.

(Kamil and Othman, 2002) [50] developed a numerical CFD model using FLUENT-CFD in order to simulate the scour around cylindrical piers. Numerical results have allowed calculating the variation of bed shear stress and thus the variation of scour depth with time.

(Khosronejad et al., 2012) [51] carried out experiments and numerical simulations to study clear water scour around three bridge piers using the FSI-CURVIB method with a k- ω closure model. One of the objectives of their study is to investigate the influence of grid resolution on the ability to predict the phenomenon by the model. The major finding is that the URANS model is not able to predict the horseshoe vortex system and the scour rate in the junction between the circular, square piers and the bed, unlike the diamond shape pier.

(Abdelaziz el al., 2010) [52] used the flow-3D code to simulated the flow field and developed a module for sediment transport in open channels. They got good agreement with experimental data, but the maximum scour depth was underestimated, and the downstream slope was over-estimated.

(Bouabdellah et al., 2018) [53] carried out a numerical simulation using a Finite Volume Method (FVM) and Detached Eddy Simulation (DES) as a turbulence model to capture the horseshoe vortex in the junction between the bed and the pier. It has been proven that the longitudinal biconcave pier shape reduces the bed shear stress at the junction between the pier and the bed by 10 % to 12 %.

4. Scour Protection System: Riprap

The principle of riprap protection is very simple: scouring occurs because the grains of soil that make up the bed is small enough to be carried away by flood currents. Suppose a mat or mass of riprap is placed on the bed around a pile. In that case, each one is heavy enough so that the most violent currents cannot move them, the materials of the bed removed from the action of the current will not be carried away, and the bed will not be scoured in the protected zone.

Experience proves that riprap, however heavy it may be, is always displaced since the level reached by the riprap against the shaft of a pile always drops with time

and must be maintained by recharging it. It is very important to understand the mechanism of this displacement. It is not the riprap on the surface of the pile that is dragged away if it has been chosen wisely heavy enough. The bed scours where the riprap stops, and the riprap slides into the ditches thus dug. They move by what the foot of their slope is ruined. The solution "riprap" presents a great variety of types of profiles and structures; however, the dimensioning always passes by definition (calculation) of the mass (or diameter) of the constituent materials (unitary block) and this, whatever the part of the work concerned.

A simple rule for choosing the size of these ripraps is to take blocks whose beginning of the movement appears for the double value of the maximum speed that can be used. The latter is usually calculated by taking the average velocity Q/S (where Q is the water flow rate and S is time). The ISBASH formula then gives the coefficient m from the driving speed, and the riprap blocks are sized as follows:

$$m = \frac{V}{\sqrt{2g\left(\frac{\gamma_s - \gamma}{\gamma}\right)d_{50}}} \quad (9)$$

With: V: the average admissible speed for the stability of the riprap

g: acceleration of gravity

γ_s : the density of the sediment

γ : density of the water

d_{50} : average diameter of the riprap

The table below allows us to define the class of riprap used for protection against scouring according to all parameters defined above

Table 2. Characteristic velocities of riprap for an average density of 2.6 t/m³

class of riprap	m	0,85	1	1,2	1,5
	d ₅₀				
1600-1500 kg	1,28	5,38	6,34	7,6	9,5
400-1600 kg	0,84	4,36	5,13	6,16	7,7
100-400 kg	0,53	3,46	4,08	4,9	6,11
25-100 kg	0,33	2,73	3,22	3,86	4,82
5-25 kg	0,2	2,13	2,5	3,00	3,76
1-5kg	0,12	1,64	1,92	2,31	2,88

5. Conclusion

The main objective of this paper is to make a comparative study of different numerical models that have been used and to cite their disadvantages and advantages. In order to use one of these models to study, the scour phenomenon and the maximum scour depth to provide techniques to combat this problem. The basic knowledge is that the DNS is very efficient to model turbulent flow, but it requires much more computing resources and more time. In LES, the contributions of the largest scales of

turbulence are computed and only the smallest structures are calculated. Concerning the solved equations, the solved quantities are filtered quantities, only the structures larger than the characteristic size of the filter are solved. The RANS simulations only need to represent the gradients present in the mean field, the rest being modelled. The main disadvantage of these methods comes from the modelling of the turbulence. The modelling is often based on simplifications which are only true under certain assumptions. The DES represent a combination between all the models and is efficient to model the turbulent flow.

Data Availability

The data used to support the findings of this study are available from the corresponding author upon request.

Funding Statement

The authors received no financial support for the research.

Acknowledgments

The authors are very grateful for all the people who contributed to the writing of this article in any way.

References

- [1] S. G. Bullard, *The Silver Bridge disaster of 1967*, Charleston, South Carolina: Arcadia Publishing, 2012.
- [2] Bernard J. Feldman, "The Collapse of the I-35W Bridge in Minneapolis," *The Physics Teacher*, vol. 48, no. 8, pp. 541-542, 2010. *Crossref*, <http://doi.org/10.1119/1.3502509>
- [3] Lu Deng, Wei Wang, and Yang Yu, "State-of-the-Art Review on the Causes and Mechanisms of Bridge Collapse," *Journal of Performance of Constructed Facilities*, vol. 30, no. 2, 2016. *Crossref*, [http://doi.org/10.1061/\(ASCE\)CF.1943-5509.0000731](http://doi.org/10.1061/(ASCE)CF.1943-5509.0000731)
- [4] J. J. Sousa et L. Bastos, "Multi-Temporal SAR Interferometry Reveals Acceleration of Bridge Sinking Before Collapse," *Natural Hazards and Earth System Sciences*, vol. 13, no. 3, pp. 659-667, 2013. *Crossref*, <http://doi.org/10.5194/nhess-13-659-2013>
- [5] Nissrine Boujia et al., "Effect of Scour on the Natural Frequency Responses of Bridge Piers: Development of a Scour Depth Sensor," *Infrastructures*, vol. 4, no. 2, p. 21, 2019. *Crossref*, <http://doi.org/10.3390/infrastructures4020021>
- [6] Hsieh W. Shen, Verne R. Schneider, and Susumu Karaki, "Local Scour around Bridge Piers," *Journal of the Hydraulics Division*, vol. 95, no. 6, pp. 1919-1940, 1969. *Crossref*, <http://doi.org/10.1061/JYCEAJ.0002197>
- [7] D. M. Sheppard, B. Melville, and H. Demir, "Evaluation of Existing Equations for Local Scour at Bridge Piers," *Journal of Hydraulic Engineering*, vol. 140, no. 1, pp. 14-23, 2014. *Crossref*, [http://doi.org/10.1061/\(ASCE\)HY.1943-7900.0000800](http://doi.org/10.1061/(ASCE)HY.1943-7900.0000800)
- [8] David Froehlich, Analysis of Onsite Measurements of Scour at Piers, 1988. [Online]. Available: https://www.academia.edu/28729468/Analysis_of_onsite_measurements_of_scour_at_piers
- [9] G. Dongguang, U. Pasada, and C.F. Nordin, Pier Scour Equations Used in the People's Republic of China Review and Summary. FHWA-SA-93-076, Federal Highway Administration: Washington, DC, USA, 1993. [Online]. Available: <https://rosap.nhtl.gov/view/dot/855>
- [10] M Diouri et al., Hydraulics of Water Crossing Structures, In: 2nd National Congress of the Mohamedia Route, Maroc. [Online]. Available: http://www.ampcr.ma/actes/2eme_congres_national_de_la_route/CONGRE/C7/1.05.pdf
- [11] Guemou Bouabdellah, Abdelali Seddini, and Abderrahmane Ghenim, "Numerical Investigations of the Bridge Pier Shape Influence on the Bed Shear Stress," *Electronic Journal of Geotechnical Engineering*, vol. 18, pp. 5685-5698, 2013.
- [12] Lu Zhou, *Numerical Modelling of Scour in Steady Flows*, 2017.
- [13] R. Balachandar, J. A. Kells, and R. J. Thiessen, "The Effect of Tailwater Depth on the Dynamics of Local Scour," *Canadian Journal of Civil Engineering*, vol. 27, no. 1, pp. 138-150, 2000. *Crossref*, <http://doi.org/10.1139/199-061>
- [14] H. N. C. Breusers, "Conformity and Time Scale in Two-Dimensional Local Scour".
- [15] S. S. Chatterjee, and S. N. Ghosh, "Submerged Horizontal Jet over Erodible Bed," *Journal of the Hydraulics Division*, vol. 106, no. 11, pp. 1765-1782, 1980. *Crossref*, <http://doi.org/10.1061/JYCEAJ.0005556>
- [16] S. S. Chatterjee, S. N. Ghosh, and M. Chatterjee, "Local Scour due to Submerged Horizontal Jet," *Journal of Hydraulic Engineering*, vol. 120, no. 8, pp. 973-992, 1994. *Crossref*, [http://doi.org/10.1061/\(ASCE\)0733-9429\(1994\)120:8\(973\)](http://doi.org/10.1061/(ASCE)0733-9429(1994)120:8(973))
- [17] Snehal C. Kapse, and Dr. R.R. Arakerimath, "CFD Analysis & Optimisation Parametric Study on Heat Transfer Enhancement by various shapes of wings and Materials with Forced Convection," *SSRG International Journal of Mechanical Engineering*, vol. 1, no. 8, pp. 1-3, 2014. *Crossref*, <https://doi.org/10.14445/23488360/IJME-V1I8P101>
- [18] Siow-Yong Lim, "Equilibrium Clear-Water Scour around an Abutment," *Journal of Hydraulic Engineering*, vol. 123, no. 3, pp. 237-243, 1997. *Crossref*, [http://doi.org/10.1061/\(ASCE\)0733-9429\(1997\)123:3\(237\)](http://doi.org/10.1061/(ASCE)0733-9429(1997)123:3(237))
- [19] U. C. Kothiyari, K. G. Ranga Raju, and R. J. Garde, "Live-Bed Scour around Cylindrical Bridge Piers," *Journal of Hydraulic Research*, vol. 30, no. 5, pp. 701-715, 1992. *Crossref*, <http://doi.org/10.1080/00221689209498889>
- [20] Bruce W. Melville, and Stephen E. Coleman, *Bridge Scour*, Highlands Ranch, Colo: Water Resources Publications, 2000.
- [21] Bruce W. Melville, "Pier and Abutment Scour: Integrated Approach," *Journal of Hydraulic Engineering*, vol. 123, no. 2, pp. 125-136, 1997. *Crossref*, [http://doi.org/10.1061/\(ASCE\)0733-9429\(1997\)123:2\(125\)](http://doi.org/10.1061/(ASCE)0733-9429(1997)123:2(125))
- [22] B. W. Melville, and A. J. Sutherland, "Design Method for Local Scour at Bridge Piers," *Journal of Hydraulic Engineering*, vol. 114, no. 10, pp. 1210-1226, 1988. *Crossref*, [http://doi.org/10.1061/\(ASCE\)0733-9429\(1988\)114:10\(1210\)](http://doi.org/10.1061/(ASCE)0733-9429(1988)114:10(1210))
- [23] L. C. van Rijn, *Local Scour near Structures*, 2018.
- [24] Richard J. S. Whitehouse, "Marine Scour at Large Foundations."

- [25] H. N. C. Breusers, G. Nicollet, et H. W. Shen, "Local Scour Around Cylindrical Piers," *Journal of Hydraulic Research*, vol. 15, no. 3, pp. 211-252, 1977. *Crossref*, <http://doi.org/10.1080/00221687709499645>
- [26] Suliman Alfarawi, Azeldin El-sawi, and Hossin Omar, "Discontinuous Finite Element Analysis of Counter Flow Heat Exchanger Unit Cell," *SSRG International Journal of Mechanical Engineering*, vol. 8, no. 8, pp. 7-10, 2021. *Crossref*, <https://doi.org/10.14445/23488360/IJME-V8I8P102>
- [27] B. M. Sumer, and J. Fredsøe, "Wave Scour around Group of Vertical Piles," *Journal of Waterway, Port, Coastal, and Ocean Engineering*, vol. 124, no. 5, pp. 248-256, 1998. *Crossref*, [https://doi.org/10.1061/\(ASCE\)0733-950X\(1998\)124:5\(248\)](https://doi.org/10.1061/(ASCE)0733-950X(1998)124:5(248))
- [28] B. Mutlu Sumer, and Jørgen Fredsøe, "Scour around Pile in Combined Waves and Current," *Journal of Hydraulic Engineering*, vol. 127, no. 5, pp. 403-411, 2001. *Crossref*, [http://doi.org/10.1061/\(ASCE\)0733-9429\(2001\)127:5\(403\)](http://doi.org/10.1061/(ASCE)0733-9429(2001)127:5(403))
- [29] Yaru Li et al., "Development of a New 3d Euler-Lagrange Model for the Prediction of Scour around Offshore Structures," *Coastal Engineering*, vol. 1, no. 34, p. 31, 2014. *Crossref*, <http://doi.org/10.9753/icce.v34.sediment.31>
- [30] Rui Sun, and Heng Xiao, "SediFoam: A General-Purpose, Open-Source CFD-DEM Solver for Particle-Laden Flow with Emphasis on Sediment Transport," *Computers & Geosciences*, vol. 89, pp. 207-219, 2016. *Crossref*, <http://doi.org/10.1016/j.cageo.2016.01.011>
- [31] Justin R. Finn, Ming Li, and Sourabh V. Apte, "Particle Based Modelling and Simulation of Natural Sand Dynamics in the Wave Bottom Boundary Layer," *Journal of Fluid Mechanics*, vol. 796, pp. 340-385, 2016. *Crossref*, <http://doi.org/10.1017/jfm.2016.246>
- [32] Xin Chen et al., "A General Two-Phase Turbulent Flow Model Applied to the Study of Sediment Transport in Open Channels," *International Journal of Multiphase Flow*, vol. 37, no. 9, pp. 1099-1108, 2011. *Crossref*, <http://doi.org/10.1016/j.ijmultiphaseflow.2011.05.013>
- [33] Sanjeev K. Jha, and Fabián A. Bombardelli, "Toward Two-Phase Flow Modeling of Nondilute Sediment Transport in Open Channels," *Journal of Geophysical Research*, vol. 115, no. F3, 2010. *Crossref*, <http://doi.org/10.1029/2009JF001347>
- [34] Ming Li, Shunqi Pan, and Brian A. O'Connor, "A Two-Phase Numerical Model for Sediment Transport Prediction under Oscillatory Sheet Flows," *Coastal Engineering*, vol. 55, no. 12, pp. 1159-1173, 2008. *Crossref*, <http://doi.org/10.1016/j.coastaleng.2008.05.003>
- [35] Dongfang Liang, Liang Cheng, and Fangjun Li, "Numerical Modeling of Flow and Scour below a Pipeline in Currents," *Coastal Engineering*, vol. 52, no. 1, pp. 43-62, 2005. *Crossref*, <http://doi.org/10.1016/j.coastaleng.2004.09.001>
- [36] Andreas Roulund et al., "Numerical and Experimental Investigation of Flow and Scour Around a Circular Pile," *Journal of Fluid Mechanics*, vol. 534, pp. 351-401, 2005. *Crossref*, <http://doi.org/10.1017/S0022112005004507>
- [37] Guemou Bouabdellah, "Study and Modeling of Scour Around Bridge Piles," PhD thesis, Abou Bekr Belkaid University, Tlemcan, Algérie, 2016.
- [38] Steven A. Orszag, "Analytical Theories of Turbulence," *Journal of Fluid Mechanics*, vol. 41, no. 2, pp. 363-386, 1970. *Crossref*, <http://doi.org/10.1017/S0022112070000642>
- [39] J.G. Wissink, and W. Rodi, "Numerical Study of the Near Wake of a Circular Cylinder," *International Journal of Heat and Fluid Flow*, vol. 29, no. 4, pp. 1060-1070, 2008. *Crossref*, <http://doi.org/10.1016/j.ijheatfluidflow.2008.04.001>
- [40] Jasmininder Singh et al., "Study of NACA 4412 and Selig 1223 Airfoils through Computational Fluid Dynamics," *SSRG International Journal of Mechanical Engineering*, vol. 2, no. 6, pp. 17-21, 2015. *Crossref*, <https://doi.org/10.14445/23488360/IJME-V2I6P104>
- [41] Nobuhisa Nagata et al., "Three-Dimensional Numerical Model for Flow and Bed Deformation around River Hydraulic Structures," *Journal of Hydraulic Engineering*, vol. 131, no. 12, pp. 1074-1087, 2005. *Crossref*, [http://doi.org/10.1061/\(ASCE\)0733-9429\(2005\)131:12\(1074\)](http://doi.org/10.1061/(ASCE)0733-9429(2005)131:12(1074))
- [42] Tarek M. Salaheldin, Jasim Imran, and M. Hanif Chaudhry, "Numerical Modeling of Three-Dimensional Flow Field Around Circular Piers," *Journal of Hydraulic Engineering*, vol. 130, no. 2, pp. 91-100, 2004. *Crossref*, [http://doi.org/10.1061/\(ASCE\)0733-9429\(2004\)130:2\(91\)](http://doi.org/10.1061/(ASCE)0733-9429(2004)130:2(91))
- [43] Philippe R. Spalart, "Detached-Eddy Simulation," *Annual Review of Fluid Mechanics*, vol. 41, no. 1, pp. 181-202, 2009. *Crossref*, <http://doi.org/10.1146/annurev.fluid.010908.165130>
- [44] Mahalakshmaiah Vaddani Dr.V.Krishnareddy, "CFD Analysis of Variable Helical Inlet Port for a Six Cylinder Engine," *SSRG International Journal of Mechanical Engineering*, vol. 1, no. 6, pp. 16-21, 2014. *Crossref*, <https://doi.org/10.14445/23488360/IJME-V1I6P107>
- [45] John E. Richardson, and Vijay G. Panchang, "Three-Dimensional Simulation of Scour-Inducing Flow at Bridge Piers," *Journal of Hydraulic Engineering*, vol. 124, no. 5, pp. 530-540, 1998. *Crossref*, [http://doi.org/10.1061/\(ASCE\)0733-9429\(1998\)124:5\(530\)](http://doi.org/10.1061/(ASCE)0733-9429(1998)124:5(530))
- [46] B. Brørs, "Numerical Modeling of Flow and Scour at Pipelines," *Journal of Hydraulic Engineering*, vol. 125, no. 5, pp. 511-523, 1999. *Crossref*, [http://doi.org/10.1061/\(ASCE\)0733-9429\(1999\)125:5\(511\)](http://doi.org/10.1061/(ASCE)0733-9429(1999)125:5(511))
- [47] Nguyen Viet Thanh, Dang Huu Chung, and Tran Dinh Nghien, "Prediction of the Local Scour at the Bridge Square Pier Using a 3D Numerical Model," *Open Journal of Applied Sciences*, vol. 04, no. 2, pp. 34-42, 2014. *Crossref*, <http://doi.org/10.4236/ojapps.2014.42005>
- [48] Ming-Hseng Tseng, Chin-Lien Yen, and Charles C. S. Song, "Computation of Three-Dimensional Flow around Square and Circular Piers," *International Journal of Numerical Methods Fluids*, vol. 34, no. 3, pp. 207-227, 2000. *Crossref*, [http://doi.org/10.1002/1097-0363\(20001015\)34:3<207::AID-FLD31>3.0.CO;2-R](http://doi.org/10.1002/1097-0363(20001015)34:3<207::AID-FLD31>3.0.CO;2-R)

- [49] [Online]. Available: 2002_icsf-1_Roulund_Sumer_Fredsoe_Michelsen_795-809.pdf
- [50] Kamil H. M. Ali, and Othman Karim, "Simulation of Flow around Piers," *Journal of Hydraulic Research*, vol. 40, no. 2, pp. 161-174, 2002. *Crossref*, <http://doi.org/10.1080/00221680209499859>
- [51] Ali Khosronejad, Seokkoo Kang, and Fotis Sotiropoulos, "Experimental and Computational Investigation of Local Scour Around Bridge Piers," *Advances in Water Resources*, vol. 37, pp. 73-85, 2012. *Crossref*, <http://doi.org/10.1016/j.advwatres.2011.09.013>
- [52] S. Abdelaziz, M. D. Bui, and P. Rutschmann, "Numerical Simulation of Scour Development due to Submerged Horizontal Jet," Bundesanstalt für Wasserbau, 2010.
- [53] B. Guemou, A. Seddini, and A. N. Ghenim, "Scour around Bridge Piers: Numerical Investigations of the Longitudinal Biconcave Pier Shape," *Periodica Polytechnica Mechanical Engineering*, vol. 62, no. 4, pp. 298-304, 2018. *Crossref*, <http://doi.org/10.3311/PPme.12263>
- [54] Arvind Prabhakar, "CFD Analysis of Static Pressure and Dynamic Pressure for Naca 4412," *International Journal of Engineering Trends and Technology*, vol. 4, no. 8, pp. 3258-3265, 2013.
- [55] Asem AL Jarrah, "CFD Study of the Normal Force Exerted on a Sphere Moving Close to a Surface," *SSRG International Journal of Chemical Engineering Research*, vol. 3, no. 1, pp. 1-6, 2016. *Crossref*, <https://doi.org/10.14445/23945370/IJCER-V3I1P101>
- [56] Oscar Link, Florian Pflieger, and Ulrich Zanke, "Characteristics of Developing Scour-Holes at a Sand-Embedded Cylinder," *International Journal of Sediment Research*, vol. 23, no. 3, pp. 258-266, 2008. *Crossref*, [https://doi.org/10.1016/S1001-6279\(08\)60023-2](https://doi.org/10.1016/S1001-6279(08)60023-2)
- [57] S. Majumdar, and W. Rodi, "Three-Dimensional Computation of Flow Past Cylindrical Structures and Model Cooling Towers," *Building and Environment*, vol. 24, no. 1, pp. 3-22, 1989. *Crossref*, [https://doi.org/10.1016/0360-1323\(89\)90012-7](https://doi.org/10.1016/0360-1323(89)90012-7)
- [58] Bingchen Liang et al., "Local Scour for Vertical Piles in Steady Currents: Review of Mechanisms, Influencing Factors and Empirical Equations," *Journal of Marine Science Engineering*, vol. 8, no. 1, p. 4, 2019. *Crossref*, <https://doi.org/10.3390/jmse8010004>
- [59] Y. Aghaee, and H. Hakimzadeh, "Three Dimensional Numerical Modeling of Flow around Bridge Piers Using LES and RANS," Bundesanstalt für Wasserbau, 2010.